INTERNATIONAL JOURNAL OF
NUMERICAL ANALYSIS AND MODELING
Volume 22, Number 6, Pages 801–823

doi: 10.4208/ijnam2025-1035

A FINITE DIFFERENCE METHOD FOR AN INTERFACE PROBLEM WITH A NONLINEAR JUMP CONDITION

SO-HSIANG CHOU, CALEB KHAEMBA, AND ALICE WACHIRA

Abstract. We propose a finite difference approach to numerically solve an interface heat equation in one dimension with discontinuous conductivity and nonlinear interface condition. The discontinuous physical solution is sought among the multiple solutions of the nonlinear equation. Our method finds the approximate jump of the exact solution by two auxiliary linear problems with finite jumps. The approximate physical solution is then obtained by a weighted sum. The convergence and stability of the method are analyzed by the method of nonnegative matrices. Numerical examples are given to confirm the theory. In particular, numerical simulations are demonstrated in regards to the study of polymetric ion-selective electrodes and ion sensors.

Key words. Finite difference method, nonlinear parabolic problems, ion sensors, transmission equation.

1. Introduction

In this paper, we study the numerics associated with the following nonlinear interface parabolic problem:
(**NIPP**)
Find $u : \Omega^- \cup \Omega^+ \times [0,T] \to \mathbb{R}$ such that $u = u(x,t)$ satisfies

$$\mathcal{L}u := u_t - (\beta u_x)_x + qu = f, \quad x \in \Omega^- \cup \Omega^+, t \in (0,T] \tag{1}$$

$$u(a) = \xi(t), \quad u(b) = \eta(t), \tag{2}$$

$$[u]_\alpha = \lambda u^+ u^-, \tag{3}$$

$$[\beta u_x]_\alpha = 0, \tag{4}$$

$$u(x,0) = g(x), \quad x \in \Omega^- \cup \Omega^+. \tag{5}$$

Here α is a fixed interface point, $\Omega^- = (a,\alpha), \Omega^+ = (\alpha,b)$, the coefficient $\beta = \beta(x) > 0$ is piecewise constant:

$$\beta = \begin{cases} \beta^- & \text{on } \Omega^-, \\ \beta^+ & \text{on } \Omega^+, \end{cases} \tag{6}$$

the functions $q = q(x) \geq 0$ and $f = f(x,t)$ are assumed to be sufficiently smooth so that the solution $u(\cdot,t)$ is smooth in $\Omega^- \cup \Omega^+$ for all $t \in (0,T]$. This assumption is needed since we consider finite difference methods throughout the paper. Also note that the boundary conditions (2) are allowed to be time dependent. The parabolic problem under consideration is nonlinear when $\lambda \neq 0$ due to the interface jump condition (3) in which the jump

$$[u]_\alpha = u^+ - u^-, u^+ = \lim_{x \to \alpha^+} u(x,t), u^- = \lim_{x \to \alpha^-} u(x,t)$$

is proportional to u^+u^- with a proportionality constant λ. In (4), $[\beta u_x]_\alpha$, the jump in flux βu_x, is assumed to be zero. Problem NIPP (1)–(5) is motivated by [4] in which Hetzer and Meir presented an idealized mathematical model in the study

Received by the editors on September 8, 2024 and, accepted on March 4, 2025.
2000 *Mathematics Subject Classification.* 65N15, 65N30.

of polymetric membrane, ion-selective electrodes and ion sensors. Following [4], a schematic diagram is shown in Figure 1 where u is the concentration, $a = -a_{aq}$, $b = a_{org}, \Omega^- = I_{aq}, \Omega^+ = I_{org}$. See [4] for more details and the finite element simulations associated with the model. A review paper on how pulsed amperometric sensors work is [2]. However, for ease of reference we will also call the problem NIPP the heat equation with discontinuous conductivity and nonlinear interface jump.

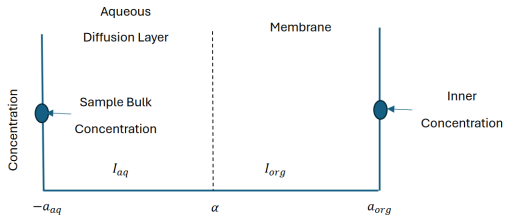

FIGURE 1. Polymeric Membrane, Ion-selective electrode, and Ion Sensor.

The $s-$parameter method. The solutions of NIPP could be obtained as follows. Let u_0 be the solution of

$$\mathcal{L}u = f, \quad x \in \Omega^- \cup \Omega^+, t \in (0, T] \tag{7}$$

$$u(a) = \xi(t), \quad u(b) = \eta(t), \tag{8}$$

$$[u]_\alpha = 0, \tag{9}$$

$$[\beta u_x]_\alpha = 0, \tag{10}$$

$$u(x, 0) = g(x), \quad x \in \Omega^- \cup \Omega^+. \tag{11}$$

On the other hand, let u_1 be the solution of

$$\mathcal{L}u = 0, \quad x \in \Omega^- \cup \Omega^+, t \in (0, T] \tag{12}$$

$$u(a) = 0, \quad u(b) = 0, \tag{13}$$

$$[u]_\alpha = 1, \tag{14}$$

$$[\beta u_x]_\alpha = 0, \tag{15}$$

$$u(x, 0) = 0, \quad x \in \Omega^- \cup \Omega^+. \tag{16}$$

We can write the general solution u of the NIPP in the form

$$u = u_0 + s u_1 \tag{17}$$

for some $s \in \mathbb{R}$. It is easy to check that (1)-(2) and (4)-(5) hold. Furthermore, the parameter $s = [u]_\alpha$ is determined by the quadratic equation induced by the condition (3) (see Eq (106)). We shall call this method the $s-$parameter method. The idea of the method can be found more or less in p. 527 of [4] without justification. Note that it can also be potentially used when dealing with the counterpart elliptic model. However, some issues needed to be resolved before it can be justified and used.

a. Are the roots s all real?
b. If so, then we have two solutions and which one will lead to a physical (concentration) solution $0 < u < 1$?
c. Furthermore, can the method be used to the discretized version of NIPP as well?

To create a discrete model, our discretization will be of the finite difference type. We propose a backward in time and central difference in space (BTCS) finite difference method to study NIPP.

The flux jump condition (4) is approximated by first order accuracy forward and backward differences at α plus a computable correction term when possible. For the elliptic model second order accuracy can always be obtained by adding a correction term while for the parabolic model, the resulting scheme will be shown to be second order in space in interesting physical cases. The same set of questions as above needs to be answered for the discrete finite difference equations as well. In the following sections, we answer these questions.

The organization of this paper is as follows. Since a parabolic equation behaves like an elliptic question after a backward discretization in time, we need to study the discrete elliptic model first. In Section 3 we address the stability and convergence of the finite difference equation for a linear elliptic model with finite jump using the nonnegative matrix theory. We then apply the $s-$parameter method to solve the nonlinear model. For an interesting role of the interface jump condition discretization, see Remark 3.5. In short, a single lower order approximation may degrade the overall accuracy in spite of the higher order approximation at non-interface points. As a consequence, a correction term is introduced to improve the local truncation error to the second order. Section 4 develops the theory for the linear parabolic case. Section 5 explains the working of the $s-$parameter method. Finally, in Section 6 we give supporting numerical results for our convergence theory. In particular, in Example 3 we explain how the physical solution is found among all possible solutions. In Example 5, we analyze an ion sensor model based on numerical simulation.

2. Finite Difference Approximations

Next, we present finite difference methods for the linear and nonlinear interface elliptic PDE and nonlinear interface parabolic PDE.

Let us define a uniform mesh on $\Omega = (a, b)$ with $a = x_0 < x_1 < \ldots < x_I < \ldots < x_{N+1} = b$ where the interface point α is located at x_I (we use a fitted mesh). The mesh size is $h = \dfrac{b-a}{N+1}$ and $x_i = a + ih, \quad i = 0, 1, \ldots, N+1$. Furthermore, define the temporal mesh size $\Delta t = \dfrac{T}{M}$ and $t_j = j\Delta t, \quad j = 0, 1, \ldots, M$, where M is a positive integer.

2.1. BTCS Approximation. We will denote by $u_{i,j} = u(x_i, t_j)$, the exact solution of (1) at the grid point (x_i, t_j), and by u_i^j, its numerical solution. The temporal derivative at (x_i, t_j) is approximated by the backward difference in time (BT)

$$u_t(x_i, t_j) \approx \frac{u_i^j - u_i^{j-1}}{\Delta t}, \tag{18}$$

where Δt represents the time step. Additionally, we approximate the spatial derivative, $(\beta u')'(x_i, t_j)$ by the central difference in space (CS), as:

$$(\beta u')'(x_i, t_j) \approx \beta(x_i) \left(\frac{-u_{i-1}^j + 2u_i^j - u_{i+1}^j}{h^2} \right). \tag{19}$$

Note that $\beta(x_i)$ is either β^- or β^+. Also, we use u' for du/dx.

2.2. Elliptic Models with linear and Non-Linear Interface Conditions. As pointed out in the Introduction section, we also need to study the elliptic model as a bridge to NIPP. In this section, we will describe the numerical solution for the elliptic problem with linear and non-linear interface condition.

First, let us consider a 1-D elliptic linear interface problem

$$-(\beta u')' + qu = f, \quad x \in \Omega^- \cup \Omega^+ = (a,\alpha) \cup (\alpha, b), \tag{20}$$

$$u(a) = \xi, \quad u(b) = \eta, \tag{21}$$

$$[u]_\alpha = \mu, \tag{22}$$

$$[\beta u']_\alpha = 0. \tag{23}$$

As before, the conductivity $\beta > 0$ is piecewise constant and $f = f(x)$. The solution u is assumed to be continuous except possibly at the interface α. We use the central difference to approximate $u''(x_i)$ so that

$$\beta u''(x_i) \approx \beta \left(\frac{-u_{i-1} + 2u_i - u_{i+1}}{h^2} \right), \qquad 1 \le i \le N, i \ne I, \tag{24}$$

where $u_i \approx u(x_i)$ and $\beta = \beta(x_i)$ is evaluated according to its position. Applying the finite difference above to (20), we have the following set of equations:

$$\begin{aligned}
&\frac{1}{h^2}\big(- u_{i-1} + 2u_i - u_{i+1}\big) + \frac{q}{\beta^-} u_i = \frac{f_i}{\beta^-}, \quad 1 \le i \le I-2, \\
&\frac{1}{h^2}\big(- u_{I-2} + 2u_{I-1} - u_I^-\big) + \frac{q}{\beta^-} u_{I-1} = \frac{f_{I-1}}{\beta^-}, \quad u_I^- \approx u(\alpha^-), \\
&\frac{1}{h^2}\big(- u_I^+ + 2u_{I+1} - u_{I+2}\big) + \frac{q}{\beta^+} u_{I+1} = \frac{f_{I+1}}{\beta^+}, \quad u_I^+ \approx u(\alpha^+), \\
&\frac{1}{h^2}\big(- u_{i-1} + 2u_i - u_{i+1}\big) + \frac{q}{\beta^+} u_i = \frac{f_i}{\beta^+}, \quad I+2 \le i \le N,
\end{aligned} \tag{25}$$

where $\alpha = x_I$ and $f_i = f(x_i)$. We will reserve the notation u_I for u_I^- and use the formula

$$u_I^+ = u_I^- + [u]_\alpha = u_I + \mu \tag{26}$$

so that our independent variables are $u_i, 1 \le i \le N$. Note that we need to impose the boundary conditions (21) on the first and Nth equations so that

$$\begin{aligned}
&\frac{1}{h^2}\big(2u_i - u_{i+1}\big) + \frac{q}{\beta^-} u_i = \frac{f_1}{\beta^-} + \frac{\xi}{h^2}, \quad i = 1, \\
&\frac{1}{h^2}\big(- u_{i-1} + 2u_i\big) + \frac{q}{\beta^+} u_i = \frac{f_N}{\beta^+} + \frac{\eta}{h^2}, \quad i = N.
\end{aligned} \tag{27}$$

At position with index $i = I$, we discretize the interface condition $[\beta u']_\alpha = 0$ using the backward difference on the left flux limit and forward difference on the right flux limit at α. Then using (26), we obtain

$$-\frac{\beta^-}{h} u_{I-1} + \frac{1}{h}\big(\beta^- + \beta^+\big) u_I - \frac{\beta^+}{h} u_{I+1} = -\frac{\beta^+}{h}\mu$$

which is obviously only a first order approximation to the flux jump condition. To achieve a possible second order approximation, we need to add a correction term C_h and the Ith equation we use is

$$-\frac{\beta^-}{h} u_{I-1} + \frac{1}{h}\big(\beta^- + \beta^+\big) u_I - \frac{\beta^+}{h} u_{I+1} = -\frac{\beta^+}{h}\mu - C_h, \tag{28}$$

where

$$C_h = \begin{cases} 0 & \text{if } q^{\pm} \neq 0 \\ -\frac{h}{2}(f^+ + f^-) & \text{if } q^{\pm} = 0. \end{cases}$$

It will be shown in (36) that (28) is a second order approximation when $q^{\pm} = 0$.

Combining (25) and (28), we arrive at a system of N linear equations in N unknowns whose matrix form is

$$A\mathbf{u} + Q_\beta \mathbf{u} = \mathbf{f}_\beta + \mathbf{u}_b \tag{29}$$

where $\mathbf{u} = (u_1, u_2, \cdots, u_N)^T$ is the unknown vector, the N by N matrix

$$A = \frac{1}{h^2}\begin{bmatrix} 2 & -1 & 0 & \cdots & \cdots & 0 & 0 \\ -1 & 2 & -1 & 0 & \cdots & & 0 \\ 0 & \ddots & \ddots & \ddots & 0 & 0 & 0 \\ 0 & 0 & -h\beta^- & h(\beta^- + \beta^+) & -h\beta^+ & 0 & 0 \\ 0 & 0 & 0 & -1 & 2 & -1 & 0 \\ & \ddots & \ddots & \ddots & \ddots & \ddots & -1 \\ & & & & & -1 & 2 \end{bmatrix}, \tag{30}$$

the N by N diagonal matrix

$$Q_\beta = diag([\frac{q_1}{\beta^-}, \ldots, \frac{q_{I-1}}{\beta^-}, 0, \frac{q_{I+1}}{\beta^+}, \ldots, \frac{q_N}{\beta^+}]), \tag{31}$$

(32)

$$\mathbf{f}_\beta := \left(\frac{f_1}{\beta^-}, \quad \frac{f_2}{\beta^-}, \quad \ldots, \quad \frac{f_{I-1}}{\beta^-}, \quad \frac{-\beta^+\mu}{h} - C_h, \quad \frac{f_{I+1}}{\beta^+} + \frac{\mu}{h^2}, \quad \ldots, \quad \frac{f_N}{\beta^+}\right)^T,$$

and the boundary contribution

$$\mathbf{u}_b = \left(\tfrac{\xi}{h^2}, \quad 0, \quad \ldots, \quad 0, \quad \tfrac{\eta}{h^2}\right)^T. \tag{33}$$

3. Consistency, Stability, and Convergence of Elliptic Problems

In this section, we examine the consistency, stability, and convergence of the linear problems.

Let $\hat{\mathbf{u}} = (u(x_1), u(x_2), \cdots, u(x_N))^T$ represent the exact solution to the elliptic problem (20)-(23) at the interior mesh points. From (29), the exact solution satisfies $A\hat{\mathbf{u}} + Q_\beta \hat{\mathbf{u}} = \mathbf{f}_\beta + \mathbf{u}_b + \tau$, where the local truncation error $\tau = (\tau_1, \tau_2, \cdots, \tau_N)^T$ can be derived as follows: for non-interface mesh point, $i \neq I$, and

$$\tau_i = \frac{1}{h^2}\big(-u_{i-1} + 2u_i - u_{i+1}\big) + \tfrac{q_i}{\beta}u_i - \tfrac{f_i}{\beta} - \tfrac{\xi}{h^2}\delta_{i1} - \tfrac{\eta}{h^2}\delta_{iN} - \tfrac{\mu}{h^2}\delta_{iI+1}, \tag{34}$$

where β is either β^+ or β^-, δ_{rs} is the Kronecker data.

At the interface ($i = I$) we have

$$\tau_I = -\frac{\beta^-}{h}u_{I-1} + \frac{1}{h}\big(\beta^- + \beta^+\big)u_I - \frac{\beta^+}{h}u_{I+1} + \frac{\beta^+}{h}\mu + C_h. \tag{35}$$

Taylor-expanding u_{I+1} and u_{I-1} around $\alpha^{\pm}$ to $\mathbb{O}(h^3)$, respectively, and using $[\beta u'] = 0$, we arrive at

$$\tau_I = \frac{1}{2}\left(-\beta^+ u''(\alpha^+) - \beta^- u''(\alpha^-)\right)h + C_h + \mathbb{O}(h^2) \tag{36}$$

$$= \frac{1}{2}\left(f^+ - q^+u^+ + f^- - q^-u^-\right)h + C_h + \mathbb{O}(h^2) \quad (\text{ by Eq.(20)}) \tag{37}$$

$$= \mathbb{O}(h^2), \tag{38}$$

if we set

$$C_h = -\frac{1}{2}\left(f^+ - q^+u^+ + f^- - q^-u^-\right)h. \tag{39}$$

Thus, a second-order LTE can be obtained in the case of $q^+ = q^- = 0$ since $C_h = -1/2(f^+ + f^-)h$ is computable. If $q^\pm \neq 0$, then we just set $C_h = 0$ so that only first-order LTE can be obtained.

Remark 3.1. *The above formula for C_h was obtained by Taylor expansion. Other approaches of obtaining correction terms are possible. For example, if we adopt the concept of virtual and real values in the immersed hybrid difference method* [5, 6]*, we would obtain a similar formula in which $C_h = f(\alpha)h$, assuming $[f]_\alpha = 0$. Notice that there is a sign difference and also our method has the interface as a mesh point, and is non-immersed.*

Remark 3.2. *We used Eq.* (20) *to replace the $-\beta u''$ terms in the elliptic model, for the parabolic model an additional u_t term appears and*

$$C_h = -\frac{1}{2}\left(f^+ - u_t^+ - q^+u^+ + f^- - u_t^- - q^-u^-\right)h. \tag{40}$$

Thus, adding a nonzero correction C_h improves a method from first order to second order when $q^+ = q^- = 0$ and when we look for an attractor in which $u_t(\alpha^\pm, t) \to 0$, as t tends to infinity.

3.1. Second order convergence and stability of linear interface elliptic model with $q = 0$. In this section, we will analyze the stability for the linear elliptic model with $q = 0$. Therefore, the error vector $e_h = \hat{\mathbf{u}}_h - \mathbf{u}_h$ (we now add the subscript h to emphasize the dependency on h), satisfies the error equation

$$A_h e_h = \tau_h \tag{41}$$

and the error is related to the local truncation error as

$$e_h = A_h^{-1}\tau_h. \tag{42}$$

Thus, the stability is still defined as

Definition 3.3. *The finite difference method applied to problem* (20)-(23) *gives rise to the system (41), and is said to be stable if there exist an h_0 and a positive constant M, such that*

$$\|A_h^{-1}\| \leq M, \qquad \forall\, 0 < h \leq h_0. \tag{43}$$

The norm here is either the max norm or the discrete L^2 norm, but in this paper we concentrate on the max or L^∞ norm.

Definition 3.4. *The finite difference method is said to be consistent with the PDE, the boundary conditions and the interface conditions if the LTE(local truncation error)*

$$\|\tau_h\| = \mathbb{O}(h^p), \tag{44}$$

where $p > 0$ is an integer, i.e., there exists a constant C such that

$$\|\tau_h\| \leq Ch^p, \qquad \forall\, 0 < h \leq h_0.$$

Remark 3.5. *Note that the LTE at a non-interface point is of second order, while at the interface point it is of first order if $q \neq 0$ and of second order if $q = 0$. Thus, $||\tau_h|| = \mathbb{O}(h^p), p = 0$ or 1. It can be shown by numerical examples (cf. Example 3 in Sec. 6) that even in the case of $q = 0$ this order cannot be improved to two if we do not add a correction term. This is in contrast to the situation (cf.* [11]*)*

in which a local degradation of the LTE at a few points will not degrade the global error when the solution is globally smooth.

As shown above for the case $q = 0$ we have second order LTE. We now show that (43) holds and therefore $||e_h|| = \mathbb{O}(h^2)$.

Let Δ_h be the discrete Laplacian:

$$\Delta_h = \frac{1}{h^2}\begin{bmatrix} 2 & -1 & 0 & 0 & \dots & 0 & 0 \\ -1 & 2 & -1 & 0 & \dots & 0 & 0 \\ 0 & -1 & 2 & -1 & \dots & 0 & 0 \\ \vdots & \vdots & \vdots & \ddots & \ddots & \vdots & \vdots \\ 0 & \dots & \dots & -1 & 2 & -1 & 0 \\ 0 & \dots & \dots & 0 & -1 & 2 & -1 \\ 0 & \dots & \dots & 0 & 0 & -1 & 2 \end{bmatrix}. \tag{45}$$

We decompose the coefficient matrix A_h of the discrete elliptic model (29) represented in (30) in terms of Δ_h and a rank-one modification matrix as illustrated below. Since we assume $q = 0$,

$$A_h = \Delta_h - \begin{bmatrix} 0 & \cdots & 0 & 0 & \cdots & 0 & 0 \\ \vdots & \vdots & \vdots & \vdots & \vdots & \vdots & \vdots \\ 0 & \cdots & 0 & 0 & \cdots & 0 & 0 \\ \vdots & \vdots & (\frac{\beta^-}{h} - \frac{1}{h^2}) & (-\frac{\hat{s}}{h} + \frac{2}{h^2}) & (\frac{\beta^+}{h} - \frac{1}{h^2}) & \vdots & \vdots \\ 0 & \cdots & 0 & 0 & \cdots & 0 & 0 \\ \vdots & \vdots & \vdots & \vdots & \vdots & \vdots & \vdots \\ 0 & \cdots & 0 & 0 & \cdots & 0 & 0 \end{bmatrix}, \tag{46}$$

where $\hat{s} = \beta^+ + \beta^-$.

Let $e_I \in \mathbb{R}^{\mathbb{N}}$ be be the Ith standard unit vector defined as $e_I = (0, \dots, 1, \dots, 0)^T$, where I is the interface index. Moreover, we define

$$w_h = \left(0, \cdots, 0, (\frac{\beta^-}{h} - \frac{1}{h^2}), (-\frac{\hat{s}}{h} + \frac{2}{h^2}), (\frac{\beta^+}{h} - \frac{1}{h^2}), 0, \cdots, 0\right)^T. \tag{47}$$

We note that w_h has the good property

$$\sum_j (w_h)_j = 0, \tag{48}$$

which will be used often. Now (46) becomes

$$A_h = \Delta_h - e_I w_h^T. \tag{49}$$

Our goal is to show that A_h is invertible and that the stability condition is satisfied. We modify the classical approach of nonnegative matrices [10].

Definition 3.6. *A matrix $D \in \mathbb{R}^{N\times N}$ is inverse nonnegative if D^{-1} exists and all entries of D^{-1} are nonnegative, i.e., $(D^{-1})_{ij} \geq 0, \forall i, j \in \{1, 2, \cdots, N\}$.*

Theorem 3.7. *Let $D \in \mathbb{R}^{N\times N}$ be a matrix. Then D is inverse nonnegative if and only if $Dy \geq 0$ implies that $y \geq 0, \quad y \in \mathbb{R}^N$.*

See [10] for its proof.

Theorem 3.8. *Let A_h be the matrix in (46). Then $A_h^{-1} \geq 0 \quad \forall\, 0 < h < 1$.*

Proof. Let $y \in \mathbb{R}^n$. Suppose $A_h y \geq 0$. Our aim is to show that $y \geq 0$. Let k be the smallest index such that $y_i \geq y_k, \quad \forall 1 \leq i \leq N$. It suffices to show that $y_k \geq 0$. We will consider four cases as follows:

Case 1: Let $k = 1$. Then we have that

$$2y_1 - y_2 \geq 0, \quad \text{implying that } 2y_1 \geq y_2 \geq y_1. \tag{50}$$

therefore $y_1 \geq 0$.

Case 2: Let $k = N$. Then we have that

$$2y_N - y_{N-1} \geq 0, \quad \text{implying that } 2y_N \geq y_{N-1} \geq y_N. \tag{51}$$

hence $y_N \geq 0$.

Case 3: Let $2 \leq k \leq N-1, \quad k \neq I$.

$$-y_{k-1} + 2y_k - y_{k+1} = (y_k - y_{k-1}) + (y_k - y_{k+1}) \geq 0. \tag{52}$$

From (52) we have that $y_k = y_{k-1}$, which contradicts k being the smallest index.

Case 4: Let $k = I$. Then we have that

$$0 \leq -\beta^- y_{k-1} + (\beta^+ + \beta^-) y_k - \beta^+ y_{k+1}, \tag{53}$$

$$= \beta^-(y_k - y_{k-1}) + \beta^+(y_k - y_{k+1}) \tag{54}$$

implies that $y_{k-1} = y_k$, which is a contradiction. □

Remark 3.9. *From Theorem 3.8, we have that $A_h^{-1} \geq 0$ exists and also given that $A_h \mathbf{u}_h = \mathbf{f}_\beta + \mathbf{u}_b$ with $A_h^{-1} \geq 0$, $\mathbf{f}_\beta \geq \mathbf{0}$, and $\mathbf{u_b} \geq \mathbf{0}$, then we must have that $\mathbf{u}_h \geq 0$.*

We need a lemma to apply the Shermann-Morrison formula for finding the inverse.

Lemma 3.10. *Let $0 < h < 1$ be the mesh size and let Δ_h be the discrete Laplacian matrix in (45). Let $\alpha = x_I$ be the interface node. Then the quantity σ_h defined as*

$$\begin{aligned} \sigma_h &:= 1 - w_h^T \Delta_h^{-1} e_I \\ &= h\big(\beta^- - (\beta^- - \beta^+)\alpha\big). \end{aligned} \tag{55}$$

Furthermore,

$$\sigma_h \neq 0 \quad \text{if } \alpha \neq \frac{\beta^-}{\beta^- - \beta^+}. \tag{56}$$

Remark 3.11. *Recall that we use the fitted mesh and the interface point α is always a mesh point. Consequently,*

$$\sigma_h = Ch \text{ for some } C \text{ independent of } h. \tag{57}$$

Furthermore, if the conductivity β and interface point α have the relation $\alpha = \beta^-/(\beta^- - \beta^+)$ then we do not have a discrete FD approximation.

Proof. Without loss of generality, we assume $\Omega = (0, 1)$. The inverse of the discrete Laplacian Δ_h is well known [11] via the Green's function approach, i.e., $G_h = \Delta_h^{-1}$, where

$$(G_h)_{i,j} = \begin{cases} h(1 - x_j)x_i, & i \leq j, \\ h(1 - x_i)x_j, & i > j. \end{cases} \tag{58}$$

where $h = 1/(N+1), x_i = ih, 1 \le i, j \le N$. Note that $G_h e_I$ is the Ith column of G_h and upon multiplying the vector w_h^T by $G_h e_I$, we have

$$w_h^T G_h e_I = \begin{bmatrix} 0 \\ \vdots \\ 0 \\ \dfrac{\beta^-}{h} - \dfrac{1}{h^2} \\ -\dfrac{\hat{s}}{h} + \dfrac{2}{h^2} \\ \dfrac{\beta^+}{h} - \dfrac{1}{h^2} \\ 0 \\ \vdots \\ 0 \end{bmatrix}^T \begin{bmatrix} 0 \\ \vdots \\ 0 \\ (G_h)_{I-1,I} \\ (G_h)_{I,I} \\ (G_h)_{I+1,I} \\ 0 \\ \vdots \\ 0 \end{bmatrix}. \tag{59}$$

Replacing x_{I-1} by $x_I - h$ and x_{I+1} by $x_I + h$ in

$$w_h^T G_h e_I = (w_h)_{I-1} h\big(1-x_I\big)x_{I-1} + (w_h)_I\big(1-x_I\big)x_I + (w_h)_{I+1} h\big(1-x_{I+1}\big)x_I, \tag{60}$$

we have

$$w_h^T G_h e_I = h\big(1-x_I\big)x_I \sum_{j=I-1}^{I+1} (w_h)_j - h^2(w_h)_{I-1}(1-x_I) - h^2 x_I (w_h)_{I+1} \tag{61}$$

$$= 0 - h\big(\beta^- - \big(\beta^- - \beta^+\big)x_I\big) + 1 \qquad \text{by (48)}. \tag{62}$$

Thus, $1 - w_h^T G_h e_I = h\big(\beta^- - \big(\beta^- - \beta^+\big)x_I\big)$. □

Lemma 3.12. *Let Δ_h as in (45) and let $e_I, w_h \in \mathbb{R}^{\mathbb{N}}$ as in (47). Assume that $\sigma_h = 1 - w_h^T \Delta_h^{-1} e_I$ is nonzero. Then the following holds:*

$$(\Delta_h - e_I w_h^T)^{-1} = \Delta_h^{-1} + \frac{1}{\sigma_h} \Delta_h^{-1} e_I w_h^T \Delta_h^{-1}. \tag{63}$$

Proof. Recall the Sherman-Morrison lemma: Let $A \in \mathbb{R}^{N\times N}, u, v \in \mathbb{R}^N$, and assume that $\sigma := 1 - v^T A^{-1} u \neq 0$, then

$$(A - uv^T)^{-1} = A^{-1} + \frac{1}{\sigma} A^{-1} u v^T A^{-1}. \tag{64}$$

The assertion now follows by setting $A = \Delta_h, u = e_I, v = w_h$ in the above lemma □

Theorem 3.13. *Let A_h be the coefficient matrix in (46) of the FD equations. Then there exists a constant $C > 0$ such that*

$$\|A_h^{-1}\|_\infty \le C \quad \forall\, 0 < h < 1. \tag{65}$$

Proof. From Lemma 3.12, we have that

$$A_h^{-1} = \Delta_h^{-1} + \frac{1}{\sigma_h} \Delta_h^{-1} e_I w_h^T \Delta_h^{-1}. \tag{66}$$

From (58), it is easy to see that $\|\Delta_h^{-1}\|_\infty \le 1$. It suffices to estimate the second (rank-one) matrix. First note that for $u, v \in \mathbb{R}^N$

$$\|uv^T\|_\infty \le \|u\|_\infty \|v\|_1,$$

where $||v||_1 = \sum_1^N |v_i|$ is the vector 1-norm of v. We apply the above inequality with $u = \frac{1}{\sigma_h}\Delta_h^{-1}e_I$ and $v = \Delta_h^{-1}w_h$. Since $1/\sigma_h = \mathbb{O}(\frac{1}{h})$ and $||\Delta_h^{-1}e_I||_\infty \leq h$ by (58), we see that $\|u\|_\infty \leq C$ for all $h > 0$. To show that $||v||_1$ is uniformly bounded in h, we can proceed as in the last lemma; using (58) to compute the entries of $\Delta_h^{-1}w_h$ and deduce that

$$(\Delta_h^{-1}w_h)_i = \begin{cases} x_i(\beta^- - \beta^+)h & \text{if } 1 \leq i \leq I \\ x_I(\beta^- - \beta^+)h - \beta^- h + 1 & \text{if } i = I \\ (1 - x_i)h(\beta^+ - \beta^-) & \text{if } I + 1 \leq i \leq N. \end{cases} \tag{67}$$

For example for $1 \leq i \leq I$

$$\begin{aligned}(\Delta_h^{-1}w_h)_i &= (\Delta_h^{-1})_{i,I-1}(w_h)_{I-1} + (\Delta_h^{-1})_{i,I}(w_h)_I + (\Delta_h^{-1})_{i,I+1}(w_h)_{I+1} \\ &= h(1 - x_{I-1})x_i(w_h)_{I-1} + h(1 - x_I)x_i(w_h)_I + h(1 - x_{I+1})x_i(w_h)_{I+1} \\ &= h(1 - x_I + h)x_i(w_h)_{I-1} + h(1 - x_I)x_i(w_h)_I + h(1 - x_I - h)x_i(w_h)_{I+1} \\ &= h(1 - x_I)x_i\left((w_h)_{I-1} + (w_h)_I + (w_h)_{I+1}\right) + x_i h^2\left((w_h)_{I-1} - (w_h)_{I+1}\right) \\ &= 0 + x_i h^2\left((w_h)_{I-1} - (w_h)_{I+1}\right) \quad (\sum_j (w_h)_j = 0) \\ &= x_i(\beta^- - \beta^+)h.\end{aligned}$$

We now estimate the three contributions in (67) to $||(\Delta_h^{-1}w_h)||_1$. First recall $x_i = ih \leq 1$ and hence

$$\sum_1^{I-1} hx_i = h^2 \sum_1^{I-1} i = \frac{I(I-1)}{2}h^2 \leq 1/2$$

or

$$|\beta^- - \beta^+| \sum_1^{I-1} hx_i \leq 1/2|\beta^- - \beta^+|. \tag{68}$$

$$|x_I(\beta^- - \beta^+)h - \beta^- h + 1| \leq |\beta^- - \beta^+| + \beta^- + 1. \tag{69}$$

$$|\beta^- - \beta^+| \sum_{I+1}^{N} (1 - x_i)h \leq |\beta^- - \beta^+|Nh \leq |\beta^- - \beta^+|. \tag{70}$$

Hence, there exists a constant C such that

$$||(\Delta_h^{-1}w_h)||_1 \leq C \quad \forall\, 0 < h < 1.$$

□

3.2. Stability analysis for linear interface elliptic model with $q \neq 0$. The finite difference coefficient matrix $\tilde{A}_h \in \mathbb{R}^{N\times N}$ now takes the form

$$\tilde{A}_h = A_h + \frac{1}{\beta}\begin{bmatrix} q(x_1) & & & & & & & \\ & \ddots & & & & & & \\ & & q(x_{I-1}) & & & & & \\ & & & 0 & & & & \\ & & & & q(x_{I+1}) & & & \\ & & & & & \ddots & & \\ & & & & & & q(x_N) \end{bmatrix}, \tag{71}$$

$$= A_h + Q_h. \tag{72}$$

where $\beta > 0$ is evaluated over its corresponding interval and $q(x) \geq 0$ is a function.

Theorem 3.14. *Let $\tilde{A}_h$ be the matrix in (71). Then $\tilde{A}_h^{-1} \geq 0, \quad \forall 0 < h < 1$.*

Proof. Let $y \in \mathbb{R}^N$. Suppose $\tilde{A}y \geq 0$. We want to show that $y \geq 0$. As before, let k be the smallest index such that $y_i \geq y_k, \quad \forall 1 \leq i \leq N$. It suffices to show that $y_k \geq 0$. We will consider four cases as follows:

Let $\hat{q}(x) = q(x)/\beta(x) \geq 0$. For $k = 1$ we have that:

$$2y_1 - y_2 + h^2\hat{q}(x_1)y_1 \geq 0, \tag{73}$$

$$2y_1 + h^2\hat{q}(x_1)y_1 \geq y_2 \geq y_1, \tag{74}$$

$$(1 + h^2\hat{q}(x_1))y_1 \geq 0, \tag{75}$$

which implies that $y_1 \geq 0$. The case $k = N$ can be handled similarly.

Next, we consider the case where $k = I$. For this case, since we do not have a contribution from q, we obtain similar results as in (53):

$$0 \leq -\beta^- y_{k-1} + (\beta^+ + \beta^-)y_k - \beta^+ y_{k+1}, \tag{76}$$

$$= -\beta^-(y_k - y_{k-1}) + \beta^+(y_k - y_{k+1}). \tag{77}$$

implies that $y_{k-1} = y_k$, which is a contradiction. Lastly, we consider $2 \leq k \leq N - 1, k \neq I$:

$$-y_{k-1} + 2y_k - y_{k+1} + h^2\hat{q}(x_k)y_k \geq 0. \tag{78}$$

using $-y_k \geq -y_{k-1}$ and $-y_k \geq -y_{k+1}$ on (78) above, we have that

$$-y_k + 2y_k - y_k + h^2\hat{q}(x_k)y_k \geq 0. \tag{79}$$

Therefore, $y_k \geq 0$ for all cases. □

Theorem 3.15. *Let $\tilde{A}_h$ be the matrix in (71). Then there exists a constant $C_2 > 0$ such that*

$$\|\tilde{A}_h^{-1}\|_\infty \leq C_2 \quad \forall 0 < h < 1. \tag{80}$$

Proof. From (72) we have $\tilde{A}_h - A_h = Q_h$, and so

$$\tilde{A}_h^{-1} - A_h^{-1} = -\tilde{A}_h^{-1}\big(\tilde{A}_h = -A_h\big)A_h^{-1} = -\tilde{A}_h^{-1}Q_hA_h^{-1} \leq 0, \tag{81}$$

where we have used Theorem 3.14 and Theorem 3.8 and $Q_h \geq 0$. Consequently, $0 \leq \tilde{A}_h^{-1} \leq A_h^{-1}$. Hence by (65)

$$\|\tilde{A}_h^{-1}\|_\infty \leq \|A_h^{-1}\|_\infty \leq C \quad \forall 0 < h < 1 \tag{82}$$

and we are done. □

4. Stability analysis for linear interface parabolic model

Now consider the parabolic problem

$$u_t - (\beta u')' + qu = f, \quad x \in \Omega^- \cup \Omega^+ = (a, \alpha) \cup (\alpha, b), \tag{83}$$

$$u(a) = \xi, \quad u(b) = \eta, \tag{84}$$

$$[u]_\alpha = \mu, \tag{85}$$

$$[\beta u']_\alpha = 0, \tag{86}$$

$$u(x, 0) = h(x). \tag{87}$$

This solution at the mesh points is expressed as $\hat{u}^j = \big(u(x_1,t_j), u(x_2,t_j), \ldots, u(x_N,t_j)\big)^T$. For simplicity, we will assume that $f = 0$, $q = 0$. The implicit finite difference method (BTCS) for the non-interface position becomes:

(88)
$$\frac{u_i^{j+1} - u_i^j}{k} + \beta_i \frac{-u_{i-1}^{j+1} + 2u_i^{j+1} - u_{i+1}^{j+1}}{h^2} = \delta_{iI+1}\frac{\beta^+\mu}{h^2}, \quad 1 \le i \le N, i \ne I \quad 0 \le j \le M.$$

We will apply the techniques used to prove the stability for elliptic problems to investigate the stability issues of the BTCS method for parabolic problems. To this end let us rearrange (88) as follows:

$$\begin{aligned} &\frac{1}{h^2}\big(-u_{i-1}^{j+1} + 2u_i^{j+1} - u_{i+1}^{j+1}\big) + \frac{1}{\beta_i k}u_i^{j+1} \\ &= \frac{1}{\beta_i k}u_i^j + \delta_{iI+1}\frac{\mu}{h^2}, \quad 1 \le i \le N, i \ne I, \quad 0 \le j \le M. \end{aligned} \tag{89}$$

At position with index $i = I$, we discretize the interface condition $[\beta u']_\alpha = 0$ as in the elliptic case we obtain the Ith equation:

$$-\frac{\beta^-}{h}u_{I-1}^{j+1} + \frac{1}{h}\big(\beta^- + \beta^+\big)u_I^{j+1} - \frac{\beta^+}{h}u_{I+1}^{j+1} = -\frac{\beta^+}{h}\mu - C_h. \tag{90}$$

By incorporating (90) into (89), we arrive at a system of N linear equations in N unknowns whose matrix form is

$$\tilde{A}_h u^{j+1} := A_h u^{j+1} + Q_\beta u^{j+1} = F^j + u_b, \tag{91}$$

where $u^{j+1} = (u_1^{j+1}, u_2^{j+1}, \cdots, u_N^{j+1})^T$ is the unknown vector, the N by N matrix

$$A_h = \frac{1}{h^2}\begin{bmatrix} 2 & -1 & 0 & \cdots & \cdots & 0 & 0 \\ -1 & 2 & -1 & 0 & \cdots & & 0 \\ 0 & \ddots & \ddots & \ddots & 0 & 0 & 0 \\ 0 & 0 & -h\beta^- & h(\beta^- + \beta^+) & -h\beta^+ & 0 & 0 \\ 0 & 0 & 0 & -1 & 2 & -1 & 0 \\ & \ddots & \ddots & \ddots & \ddots & \ddots & -1 \\ & & & & & -1 & 2 \end{bmatrix}, \tag{92}$$

the N by N diagonal matrix

$$Q_\beta = diag([\frac{1}{\beta^- k}, \ldots, \frac{1}{\beta^- k}, 0, \frac{1}{\beta^+ k}, \ldots, \frac{1}{\beta^+ k}]), \tag{93}$$

(94)
$$F^j = \left(\frac{f_1}{\beta^- k} \quad \frac{f_2}{\beta^- k} \quad \ldots \quad \frac{f_{I-1}}{\beta^- k} \quad \frac{-\beta^+\mu}{h} - C_h \quad \frac{f_{I+1}}{\beta^+ k} + \frac{\mu}{h^2} \quad \ldots \quad \frac{f_N}{\beta^+ k},\right)^T, f_i = u_i^j$$

$$u_b = \big(\tfrac{\xi}{h^2}, \quad 0, \quad \ldots \quad 0, \quad \tfrac{\eta}{h^2}\big)^T. \tag{95}$$

We thus have all the stability and nonnegativity results inherited from the elliptic case.

Theorem 4.1. *Consider the BTCS method* (91)*. We see that* $\tilde{A}_h$ *and* A_h *are invertible and there exist* h_0 *and a positive constant* C *such that*

$$||\tilde{A}_h^{-1}||_\infty \le C \text{ and } ||A_h^{-1}||_\infty \le C \quad \forall\, 0 < h \le h_0. \tag{96}$$

Next, we define the local truncation error $\frac{1}{\beta}\tau_{h,i}^{j}(u)$ at time t_j and x_i where the classical local truncation error

$$\tau_{h,i}^{j+1} := \frac{u_i^{j+1}-u_i^j}{k} - \frac{\beta}{h^2}\big(-u_{i-1}^{j+1}+2u_i^{j+1}-u_{i+1}^{j+1}\big) + \delta_{iI+1}\frac{\beta^+\mu}{h^2}, \qquad 1\le i\le N, i\ne I, 0\le j\le M. \tag{97}$$

It is well known [13] that at the interior points of the domain that $\tau_{h,k}^{j+1} = \mathbb{O}(k+h^2)$, and at the interface point the jump condition does not depend on time, and so the technique of deriving the LTE is similar to the ones used in (36). Consequently, the LTE satisfies

$$\tau = \mathbb{O}(k+h^p), p = 1 \text{ or } 2. \tag{98}$$

By the Lax equivalence theorem, we have the convergence of the BTCS scheme.

5. The $s-$parameter method for nonlinear models

In this section we show how to solve nonlinear elliptic and parabolic models using the $s-$parameter method. Our nonlinear elliptic model is

$$-(\beta u')' + qu = f, \quad x\in\Omega^-\cup\Omega^+ = (a,\alpha)\cup(\alpha,b), \tag{99}$$

$$u(a)=\xi, \quad u(b)=\eta, \tag{100}$$

$$[u]_\alpha = \lambda u^+u^-, \lambda\ne 0, \tag{101}$$

$$[\beta u']_\alpha = 0. \tag{102}$$

This model has multiple solutions, and in practice we are only interested in the physical (concentration) solution $0<u<1$, see Example 3 in the next section for further discussion. With reference to the linear model (20)-(23), notice that its solution depends on the data set $\mathbb{D} := \{f,\xi,\eta,\mu\}$ with q and β being fixed. We let

$$u_1 \text{ be the solution with } \mathbb{D} := \{0,0,0,\mu=1\}, \tag{103}$$

$$u_0 \text{ be the solution with } \mathbb{D} := \{f,\xi,\eta,\mu=0\}. \tag{104}$$

In the $s-$parameter method we look for the solution to the nonlinear model (99)-(102) in the form

$$u = u_0 + su_1. \tag{105}$$

Note that the parameter $s=[u]_\alpha$ and is determined by (101) through the quadratic equation

$$a_2s^2 + a_1s + a_0 = 0, \tag{106}$$

$$a_2 = \lambda u_1^+u_1^-, \tag{107}$$

$$a_1 = \lambda(u_0^+u_1^- + u_1^+u_0^-) - 1, \tag{108}$$

$$a_0 = \lambda u_0^+u_0^-. \tag{109}$$

Thus, the nonlinear model has a solution only if the discriminant

$$\Delta = a_1^2 - 4a_2a_0 = r^2 - 4\lambda u_1^+u_0^- \ge 0, \quad r := \lambda(u_0^+u_1^- - u_1^+u_0^-) - 1. \tag{110}$$

In the general code, this condition needs to be monitored. However, for the important case of the ion sensor problem (ISE) [4], the parameter λ is always negative (*Caution*: in [4] the quantity $[u]_\alpha$ is defined as $u^- - u^+$ instead of $u^+ - u^-$) and $u_0\ge 0$ (concentration or by the maximal principle via the boundary condition), so the last term $-4\lambda u_1^+u_0^-$ is always nonnegative once we can show $u_1^+ > 0$. To do so, note that when β is piecewise constant, the steady state of u_1 can be analytically

found to be piecewise linear, and $u_1^+ > 0$ since the ratio $\beta^+/\beta^- > 0$ (see Example 1 and Fig. 2 below). Let us turn to the nonlinear parabolic model NIPP (1)- (5). The data set $\mathbb{D}$ now includes the initial profile and for a given function $h = h(x)$ we can define

$$u_1 \text{ be the solution with } \mathbb{D} := \{0, 0, 0, \mu = 1, h\} \tag{111}$$

$$u_0 \text{ be the solution with } \mathbb{D} := \{f, \xi, \eta, \mu = 0, g - s_0 h\}, \tag{112}$$

where $s_0 = g^+ - g^-$, the jump of the initial profile. First, note that when β is piecewise constant, $u_1(x, \infty)$, the steady state of u_1, is u_1 in the elliptic case. If we choose $h(x) = u_1(x, \infty)$, because of the uniqueness [8, 9, 15], it is also the solution of the parabolic problem (111). Thus, we see that $u_1^+ > 0$ for all times.

6. Numerical Experiments

In this section, we present two groups of numerical results, one for elliptic models and one for parabolic models. The first two or one numerical experiment(s) of each group is always for the linear case. The third one then demonstrates the results for the non-linear cases using the $s-$parameter method. The order of accuracy for the linear cases is always first order in time and second order in space according to the theory proved in the previous sections.

Example 1. Linear Elliptic Model

We consider a linear interface elliptic problem in the domain $[-1, 1]$, with $\alpha = 0$, $[u]_\alpha = \mu = 1$, and $[\beta u']_\alpha = 0$ together with

$$-(\beta u')' = 0, \quad x \in [-1, 1], \tag{113}$$

$$u(-1) = u(1) = 0. \tag{114}$$

Let $r = \beta^+/\beta^-$. Note that the exact solution u is the function u_1 in the previous sections:

$$u(x) = \begin{cases} -\frac{r}{1+r}(x+1) & -1 \le x \le 0, \\ -\frac{1}{1+r}(x-1) & 0 < x \le 1. \end{cases} \tag{115}$$

It has the physical property $1 > u^+ = 1/(1+r) > 0$.

For the physical problems that are of interest [2], the ratio r is usually between zero and one. So, we run this problem with $\beta^- = 1, \beta^+ = 0.1$ and the related numerical results are presented below.

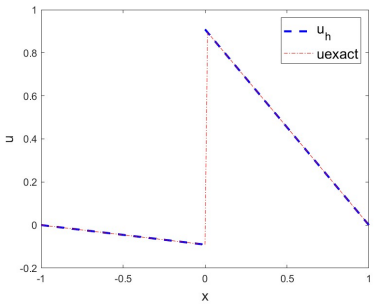

FIGURE 2. Numerical solution u_h and exact solution u with $h = 0.125$ (example 1).

Figure 2 displays both the exact solution and the approximate solution. It is evident that they are indistinguishable at each mesh point. Let the maximum norm error

$$e_h := \max_{0\le i\le N+1} |u_h(x_i)-u(x_i)|, N = 2MR-1, x_i = a+ih, h = (b-a)/(N+1), \tag{116}$$

where MR is the number of subintervals from the interface point α to the right endpoint b. We report the maximum norm error in Table 1. Note that u_h has machine precision error.

TABLE 1. L_∞ error (example 1).

MR	h	L_∞
4	0.25	2.4980 e -16
8	0.125	5.8287 e -16
16	0.0625	1.7764 e -15
32	0.03125	5.9258 e -15
64	0.015625	7.8132 e -15

Example 2. Linear Elliptic Model

This time we try a linear interface elliptic problem with an oscillatory load.

$$-(\beta u')' = 0.1\sin(\pi x), \quad -1 \le x \le 1, \tag{117}$$

$$u(-1) = u(1) = 0, \tag{118}$$

$[u]_\alpha = 1.1, \alpha = 0$ and $\beta^- = 1, \beta^+ = 0.1$. The exact solution

$$u(x) = \begin{cases} \frac{0.1}{\pi^2}\sin(\pi x) - 0.1(x+1) & -1 \le x \le 0, \\ \frac{1}{\pi^2}\sin(\pi x) - (x-1) & 0 < x \le 1. \end{cases} \tag{119}$$

The numerical results are in Table 2 and Fig. 3. Throughout this section, the

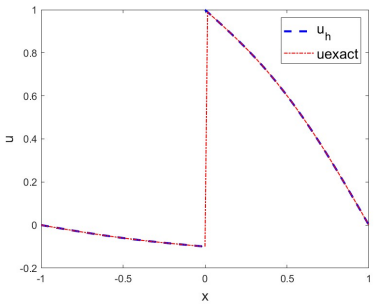

FIGURE 3. Numerical solution u_h and exact solution u with $h = 0.125$ (example 2).

error ratio is defined as

$$\text{Error Ratio} := e_h/e_{2h}. \tag{120}$$

Table 2 shows that the method is second-order since the error is reduced by a quarter when h is halved.

TABLE 2. Table for L_∞ errors (example 2).

MR	h	L_∞	Error Ratio	Order
4	0.25	5.3730e-03	0.22691	≈ 2
8	0.125	1.3122e-03	0.24422	≈ 2
16	0.0625	3.2615e-04	0.24655	≈ 2
32	0.03125	8.1419e-05	0.24964	≈ 2
64	0.015625	2.0348e-05	0.24991	≈ 2

Example 3. Nonlinear Elliptic Model

Now we consider a non-linear interface elliptic problem:

$$-(\beta u')' = 1, \quad -1 \le x \le 1, \tag{121}$$

$$u(-1) = u(1) = 0, \tag{122}$$

whose jump conditions at $\alpha = 0$ are given by

$$[u]_\alpha = \lambda u^+ u^-, \tag{123}$$

$$[\beta u']_\alpha = 0 \tag{124}$$

and the conductivity is $\beta^- = 2$ and $\beta^+ = 1$. The exact solution is of the form

$$u(x) = \begin{cases} -0.25(x+1)^2 + B(x+1) & -1 \le x \le 0, \\ -0.5(x-1)^2 + C(x-1) & 0 < x \le 1. \end{cases} \tag{125}$$

By (124) we have

$$C = 2B - 2,$$

which leads to a quadratic equation through (123). More specifically

$$2B^2 - (2+3\gamma)B + \frac{3}{8} + \frac{7}{4}\gamma = 0, \ \gamma = 1/\lambda$$

or

$$B = \frac{2 + 3\gamma \pm \sqrt{(2+3\gamma)^2 - (3+14\gamma)}}{4}.$$

Thus, we always have two real solutions since the discriminant $\Delta = 9\gamma^2 - 2\gamma + 1 = ((\lambda-1)^2 + 8)/\lambda^2 > 0$.

To sort out the physical solution, we require $0 < u < 1$, which leads to $B \ge 1/4$ and $C \le -1/2$. Combining with $C = 2B - 2$, we conclude that for u to be physical, we must have

$$\frac{1}{4} \le B \le \frac{3}{4}. \tag{126}$$

Let us look at a few cases:
Case 1. $\lambda = 3$ so that $B = \frac{2 \pm \sqrt{3}/3}{4}$. Checking against (126), we see that only the plus sign gives the physical solution.
Case 2. $\lambda = -2$ so that $B = \frac{0.5 \pm \sqrt{17}/2}{4}$, of which only the positive sign gives the physical solution.
Case 3. $\lambda = 2$ so that $B = \frac{3.5 \pm 3/2}{4}$. The positive sign solution u_P does not satisfy (126). Thus, only the negative sign solution u_N is physical.

We will set $\lambda = -2.5$ so that

$$B = \frac{\sqrt{81} + 4}{20}, \quad C = 2B - 2. \tag{127}$$

The numerical results for this case are given below. In Fig. 4, the numerical method

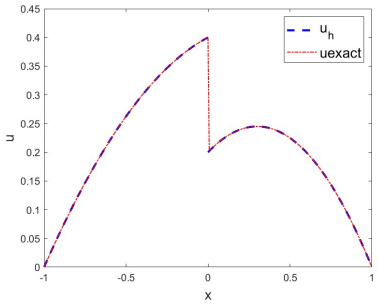

FIGURE 4. Numerical solution u_h and exact solution u with $h = 0.125$ (example 3).

captures the behavior of the exact solution since the two curves coincide.

TABLE 3. L_∞ errors **without** correction term C_h (example 3).

MR	h	L_∞ Error	L_∞ Error Ratio	Order
8	0.125	0.055103	0.50463	≈ 1
16	0.0625	0.027668	0.50211	≈ 1
32	0.03125	0.013682	0.50101	≈ 1
64	0.015625	0.0069377	0.50049	≈ 1
128	0.0078125	0.0034705	0.50024	≈ 1

TABLE 4. L_∞ errors **with correction term** C_h (example 3).

MR	h	L_∞ Error
8	0.125	2.2204e-16
16	0.0625	2.7756e-16
32	0.03125	5.6621e-15
64	0.015625	3.3307e-15
128	0.0078125	7.4385e-15

Table 3 shows that our solution achieves *only* a first-order convergence for the non-linear interface elliptic problem if the correction term is missing, i.e., $C_h = 0$. However, when the correction term is added, the second-order accuracy is achieved. Actually, we have machine precision as indicated in Table 4.

We next present results for the parabolic model.

Example 4. Linear Parabolic Model

$$u_t - (\beta u')' = f(x,t), \quad -1 \le x \le 1, t \in (0,T] \tag{128}$$

$$u(-1,t) = 0, \quad u(1,t) = 0, \tag{129}$$

$$[u]_\alpha = \mu, [\beta u']_\alpha = 0, \tag{130}$$

$$u(x,0) = u_0(x) \tag{131}$$

with $\alpha = 0$, $\mu = 2.5$, $\beta^- = 1, \beta^+ = 0.1$, the final time $T = 1$, and the right hand side

$$f(x,t) = \begin{cases} e^t \sin(\pi x) + \beta^- \pi^2 e^t \sin(\pi x) & -1 \le x \le 0, \\ re^t \sin(\pi x) + \beta^- \pi^2 e^t \sin(\pi x) & 0 < x \le 1 \end{cases} \tag{132}$$

and $r = \dfrac{\beta^-}{\beta^+} = 10$. The exact solution

$$u(x,t) = \begin{cases} e^t \sin(\pi x) + A(x+1) & -1 \le x \le 0, \\ re^t \sin(\pi x) + B(x-1) & 0 < x \le 1, \end{cases} \tag{133}$$

where

$$A = -\frac{\mu}{1+r}, \quad B = rA. \tag{134}$$

Consequently, $u_t^+ = u_t^- = 0$ and $f^+ = f^- = 0$.

Notice that there is no steady-state solution due to the e^t term. We set the final target time T to 1, a moderate number, and compare the exact and numerical solutions at T. Fig. 5 gives a good match between the exact and approximate solutions at $T = 1$. We obtain first order in time and second order in space as shown in Table 5, taking time step $k = h^2$. We also used Crank-Nicolson with $k = h$ and obtained the same result, although not reported here.

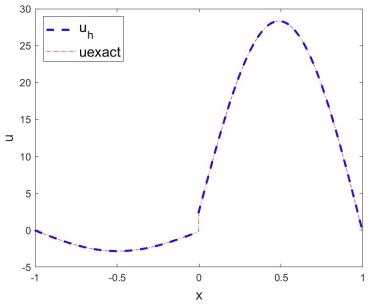

FIGURE 5. Numerical solution u_h and exact solution u with $h = 0.125$ (example 4).

TABLE 5. L_∞ errors (example 4).

MR	h	L_∞ Error	L_∞ Error Ratio	Order
8	0.125	0.65974	0.25328	≈ 2
16	0.0625	0.16552	0.25088	≈ 2
32	0.03125	0.41419	0.25024	≈ 2
64	0.015625	0.10358	0.25007	≈ 2
128	0.0078125	0.0025897	0.25002	≈ 2

Example 5. Nonlinear Parabolic Model for the Ion-Selective Electrode (ISE) problem [4, 12].

Next, we consider a non-linear interface parabolic model that models the mechanism in an ISE problem.

$$u_t - (\beta u')' = 0, \quad -1 \le x \le 1, t \in (0, T] \tag{135}$$

$$u(-1, t) = \xi(t), \quad u(1, t) = 1, \tag{136}$$

$$[\beta u'] = 0, \tag{137}$$

$$[u] = -u^+ u^-, \tag{138}$$

where $\beta^- = 1, \beta^+ = 0.1$. In reference to Fig. 1, the right boundary maintains a constant concentration of one, and the left boundary condition is evolving to the zero concentration eventually according to

$$u(-1, t) = \begin{cases} 0 & \text{if } 0 < t \le 0.2, \\ 0.5 & \text{if } 0.2 < t < 2, \\ 0 & \text{if } t > 2. \end{cases} \tag{139}$$

This problem has one and only one steady state or equilibrium solution (see Fig. 6):

$$u(x, \infty) = \begin{cases} \dfrac{-5 + \sqrt{(35)}}{10}(x + 1), & -1 \le x \le 0, \\ 1 - (5 - \sqrt{(35)}(x - 1) & 0 < x \le 1. \end{cases} \tag{140}$$

and we use it as the initial profile. With this initial profile, Hetzer and Meir [4]

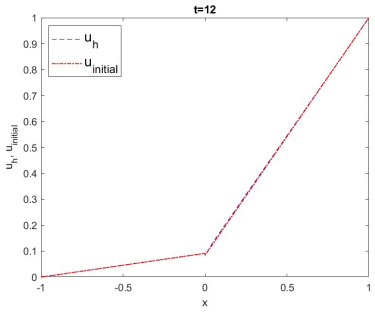

FIGURE 6. Plot of u_h at $t = 12$ against the initial profile (example 5).

used a finite element method to generate a sequence of snapshots of the approximate solution (similar to Fig. 8 below) up to the final time $T = 3.6$. However, they did not give any further analysis. Below, we fill the gap and analyze the model.

First, we want to confirm whether the above equilibrium solution is an attractor. At the interior points $u_t = \beta u_{xx}$ holds, and we can use concavity of the solution to detect if u_t is negative or not. So the source of uncertainty is on the left boundary and at the interface point, where no PDE holds. Looking at Fig. 8, at the top two subplots ($t < 0.2$), the solution stays put. At $t = 0.2$, the change of boundary condition sets in and generates a concavity near the boundary, and the left piece starts to go under a transition of downward-concavity up to $t = 2.0$. The left piece settles when $t = 3.2$. The right piece of the solution lags behind in settling because its diffusion coefficient $\beta^+ = 0.1$ is smaller.

Further examining the maximum errors $u_h(x,T) - u_h(x,0)$ at $T = 12, 24, 36$ in Tables 6 and 7, we confirm that the equilibrium solution is indeed an attractor, although the convergence is not fast. Compared with other times, at $T = 3.6$ the approximation solution $u_h(x,T)$ is not as close to $u(x,\infty)$. The evolution behavior can also be interpreted by looking at Fig. 7. At the breakpoints of the left boundary condition $t = 0.2, 2$, we see a visible transition of the error. At $t = 3.6$ the error is still a little bit away from zero. After $t = 9$ the error curve is asymptotically to zero.

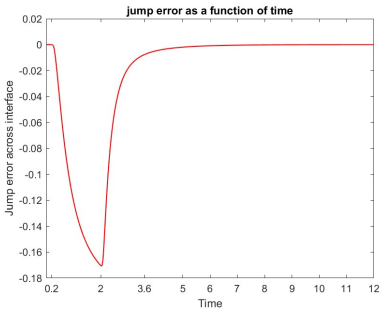

FIGURE 7. Plot of $[u_h - u]_\alpha(t)$ over time interval $[0, 12]$ (example 5).

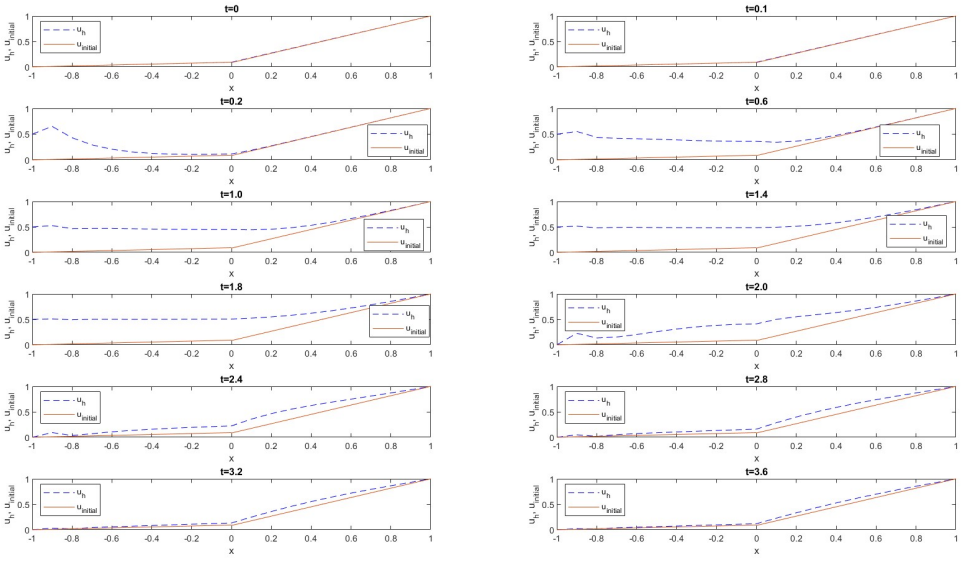

FIGURE 8. Numerical solution plotted against initial profile at various instants (example 5).

TABLE 6. Table for checking steady state (example 5).

h	L_∞ Error	Error Ratio	L_∞ Error	Error Ratios
0.025	0.018955	1.0883	3.4498e-05	1.1027
0.0125	0.013915	1.0295	2.5043e-05	1.0180
0.00625	0.0098382	0.99565	1.7949e-05	1.0093
0.003125	0.0069779	1.0009	1.2882e-05	1.0128
	Error at $T = 3.6$		Error at $T = 12$	

TABLE 7. Table for checking steady state (example 5)

h	L_∞ Error	Error Ratio	L_∞ Error	Error Ratios
0.025	3.0853e-09	1.1266	2.8177e-13	1.1759
0.0125	2.3351e-09	1.0614	2.1638e-13	1.0769
0.00625	1.7014e-09	1.0216	1.6021e-13	1.0427
0.003125	1.2225e-09	1.0139	1.1362e-13	1.0008
	Error at $T = 24$		Error at $T = 36$	

Example 6. Nonlinear parabolic model that has a steady-state solution

In the last example, the second order convergence did not carry over to the nonlinear model since the error ratios in the tables were always near one. In this example we will see that the second order convergence carries over to the nonlinear case. Consider

$$u_t - (\beta u')' = f, \quad -1 \le x \le 1, t \in (0, T_f] \tag{141}$$

$$u(-1,t) = 0, \quad u(1,t) = 1/(1-\lambda), \tag{142}$$

$$[\beta u']_\alpha = 0, \tag{143}$$

$$[u]_\alpha = \lambda u^+ u^-, \tag{144}$$

$$u(x,0) = g(x), \tag{145}$$

where $\beta^- = 1$ and $\beta^+ = 0.1$. The source term function

$$f(x,t) = \begin{cases} A\big(\gamma + \beta^- \pi^2\big) & -1 \le x \le 0, \\ rB\big(\gamma(x - x^2) + 2\beta^+\big) + 2\beta^- & 0 < x \le 1, \end{cases} \tag{146}$$

where $\gamma = -1, A = e^{\gamma t}\sin(\pi x)$ and $B = \pi e^{\gamma t}$. We set the decaying factor $\gamma = -1$ so that the problem can evolve to an equilibrium. Among the two exact solutions, we pick the one defined by

$$u(x,t) = \begin{cases} e^{\gamma t}\sin(\pi x) + x + 1 & -1 \le x \le 0, \\ \dfrac{1}{1-\lambda} + r(\pi e^{\gamma t} + 1)\big(x - x^2\big) & 0 < x \le 1. \end{cases} \tag{147}$$

to converge to. The initial profile in the numerical run is set to $g(x) = u(x,0)$. The approximate solution u_h is computed at each time by

$$u_0 + s(t)u_1, \quad 1 \le t \le T. \tag{148}$$

Fig. 9 shows that the exact and approximate solutions match well at $T_f = 2$. Furthermore, Table 8 shows second-order convergence in space. The interface jump

error $[u] - [u_h]$ at $T = 2$ with various h's also shows the second-order accuracy. Finally, the evolution of $[u] - [u_h]$ over the time interval $[0, 2]$ is shown in Fig. 10.

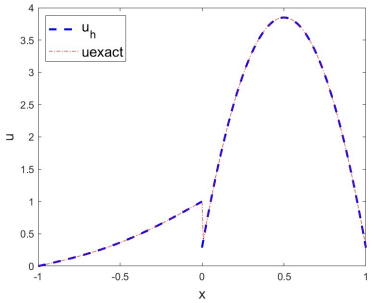

FIGURE 9. Numerical u_h and exact solution u with $h = 0.125$ (example 6).

TABLE 8. L_∞ errors and jump errors at $T = 2$ (example 6).

h	L_∞ Error	L_∞ Error Ratio	Jump Error	Jump Error Ratios
0.125	1.3724e-2	0.24556	0.0515	
0.0625	3.3703e-3	0.24558	0.0126	0.2447
0.03125	8.3265e-4	0.24705	0.0031	0.24706
0.015625	2.0673e-4	0.24827	0.0008	0.2483
0.0078125	5.1473e-5	0.24899	0.0002	0.24899

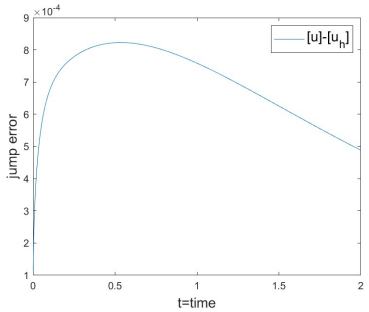

FIGURE 10. Evolution of the jump error $[u] - [u_h]$ (example 6).

7. Conclusions

Let us make a few concluding remarks about future works. Although we used the $s-$parameter method to solve the non-linear equations, Newton's method can be an alternative [14]. A refined finite element approach to the parabolic model is also possible [7]. However, as far as higher order methods are concerned combining the $s-$parameter method with the immersed interface method [3] or the enriched method [1] to solve the current nonlinear model is most promising.

Acknowledgments

The authors thank anonymous referees for their detailed and insightful comments, which have greatly improved this paper.

References

[1] C. Attanayake, S.-H. Chou, and Q. Deng, High-order enriched finite element methods for elliptic interface problems with discontinuous solutions, International Journal of Numerical Analysis and Modeling, 20 (2023), pp. 870–895.
[2] E. Bakker and A. J. Meir, How do pulsed amperometric ion sensors work? a simple pde model, SIAM Review, 45 (2003), pp. 327–344.
[3] S.-H. Chou and N. P. Fonga, An immersed interface method for parabolic interface problems with nonlinear jump condition, (2025).
[4] G. Hetzer and A. Meir, On an interface problem with a nonlinear jump condition, numerical approximation of solutions, International Journal of Numerical Analysis and Modeling, 4 (2007), pp. 519–530.
[5] Y. Jeon, An immersed hybrid difference method for the elliptic interface equation, Japan Journal of Industrial and Applied Mathematics, 39 (2022), pp. 669–692.
[6] Y. Jeon and S.-Y. Yi, The immersed interface hybridized difference method for parabolic interface problems., Numerical Mathematics: Theory, Methods & Applications, 15 (2022).
[7] C. S. Khaemba, Elliptic and parabolic interface problems with nonlinear jump condition, Master's thesis, Bowling Green State University, 2024.
[8] N. V. Krylov, Nonlinear elliptic and parabolic equations of the second order, Springer, 1987.
[9] O. A. Ladyzhenskaia, V. A. Solonnikov, and N. N. Ural'tseva, Linear and quasi-linear equations of parabolic type, vol. 23, American Mathematical Soc., 1968.
[10] H. Le Dret and B. Lucquin, Partial differential equations: modeling, analysis and numerical approximation, vol. 168, Springer, 2016.
[11] R. J. LeVeque, Finite difference methods for ordinary and partial differential equations: steady-state and time-dependent problems, SIAM, 2007.
[12] A. Radu, A. J. Meir, and E. Bakker, Dynamic diffusion model for tracing the real-time potential response of polymeric membrane ion-selective electrodes, Analytical chemistry, 76 (2004), pp. 6402–6409.
[13] G. D. Smith, Numerical solution of partial differential equations: finite difference methods, Oxford University Press, 1985.
[14] A. W. Wachira, Finite difference methods for non-linear interface elliptic and parabolic problems, Master's thesis, Bowling Green State University, 2024.
[15] S. Zhu, G. Yuan, and W. Sun, Convergence and stability of explicit/implicit schemes for parabolic equations with discontinuous coefficients, International Journal of Numerical Analysis and Modeling, 1 (2004), pp. 131–146.

Department of Mathematics and Statistics, Bowling Green State university, Bowling Green, OH, 43403-0221, USA

E-mail: chou@bgsu.edu and cskhaem@bgsu.edu and awachir@bgsu.edu